ORGANIC PROCESS RESEARCH & DEVELOPMENT
OPR&D

Communication

Process Development and Large-Scale Synthesis of BTK Inhibitor BIIB068

Chaomin Li, Lloyd Franklin, Robbie Chen, Tamera Mack, Michael Humora, Bin Ma, Brian T Hopkins, John Guzowski, Fengmei Zheng, Michael MacPhee, Yiqing Lin, Steven Ferguson, Daniel Patience, George A. Moniz, William F Kiesman, and Erin M O'Brien

Org. Process Res. Dev., **Just Accepted Manuscript** • DOI: 10.1021/acs.oprd.0c00087 • Publication Date (Web): 21 Apr 2020

Process Development and Large-Scale Synthesis of BTK Inhibitor BIIB068

Chaomin Li,* Lloyd Franklin, Robbie Chen, Tamera Mack, Michael Humora, Bin Ma, Brian T. Hopkins, John Guzowski, Fengmei Zheng, Michael MacPhee, Yiqing Lin, Steven Ferguson, Daniel Patience, George A. Moniz, William F. Kiesman, Erin M. O'Brien

Table of Contents

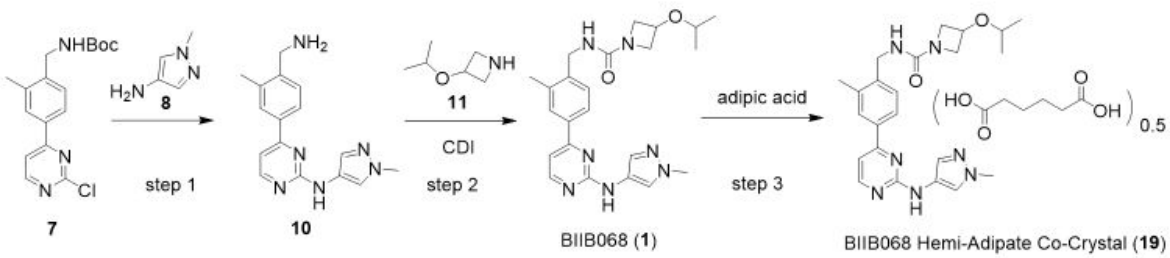

Results of BIIB068 Process Development:

- Removal of transition metal from the amination step.
- Two silica gel column chromatography operations in the original synthesis were successfully removed.
- Significantly improved the overall yield from 47% to 80% (from **7** to API) with proper impurity control.
- A reproducible process was developed to generate hemi-adipate co-crystal **19.**
- Process was scaled up to deliver 9.7 kg of high-quality API for toxicology studies and clinical trials.

Abstract:

Chemical process development efforts leading to multi-kilogram production of BIIB068 hemi-adipate will be discussed. Process optimization has resulted in 1) removal of transition metal from the process; 2) a streamlined process with significantly improved overall yield; 3) appropriate impurity control (including potential mutagenic impurities or PMI), which enabled delivery of quality material for toxicology studies and clinical trials.

Keywords: Process development, BTK inhibitor, Amination, Urea formation, Impurity control, Hemi-adipate

Introduction

Bruton's tyrosine kinase (BTK) is a cytoplasmic, non-receptor tyrosine kinase that functions downstream of the B cell receptor (BCR) in B cells and downstream of Fc receptors in myeloid cells. BTK mediates B cell receptor signaling leading to regulation of B cell activation, proliferation and differentiation. There is a strong biologic rationale for targeting diseases in which the B cell pathway is central to disease pathogenesis such as B cell mediated autoimmune diseases as well as B cell lymphoma or leukemia and atopic diseases. Ibrutinib is a clinically validated BTK inhibitor.[1] In addition, inhibition of BTK kinase activity may also provide therapeutic benefit to patients suffering from autoimmune disorders by blocking aberrant B and myeloid cell activation.[2]

As part of an ongoing research/development program at Biogen, an aminopyrazolopyrimidine compound BIIB068 (**1**), was discovered as a highly potent BTK inhibitor with good oral bioavailability, and a promising candidate for the treatment of autoimmune diseases with significantly unmet medical needs such as Systemic Lupus Erythematosus (SLE) and primary Sjögren's Syndrome (pSS).[3]

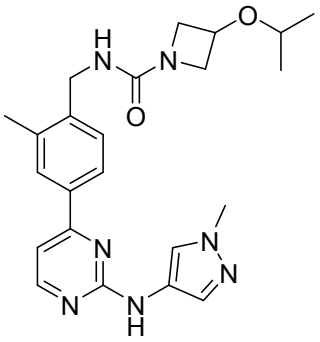

BIIB068 (1)

Figure 1. BIIB068 (**1**), a potent BTK inhibitor

While the discovery synthesis of BIIB068 was straightforward in terms of bond construction strategy, there was significant room for reaction condition improvement to enable a suitable process for large-scale production of drug substance to support preclinical and clinical studies. This article describes process development efforts that resulted in a practical and

scalable manufacturing process for multi-kilogram production of BIIB068 hemi-adipate co-crystal (**19**).

Results and Discussion

Medicinal Chemistry Synthetic Route to 1. Synthesis of **1** via the discovery route is shown in Scheme 1. Borane reduction of 4-bromo-2-methylbenzonitrile (**2**) afforded benzylamine **3** which was isolated as an HCl salt in 90 % yield. Boc protection of **3** gave **4** as a white solid which was used in the next step without further purification with 95 % yield. Aryl bromide **4** was converted to the corresponding boronate (**5**) via Miyaura borylation (69 % yield). Subsequent Suzuki reaction of boronate **5** with 2,4-dichloropyrimidine (**6**) delivered biaryl intermediate **7** in 80% yield after silica gel column purification. A transition metal catalyzed C-N coupling of **7** with 1-methyl-1*H*-pyrazol-4-amine (**8**) was then applied to install the aminopyrazole moiety and the C-N coupling product **9** was isolated in 63% yield using chromatography. The Boc protecting group in **9** was successfully removed using HCl in MeOH to liberate the amino group and deliver benzylamine **10** in 90 % yield. The last chemical transformation step in the 1 synthesis involved urea formation with 3-isopropoxyazetidine (**11**) using CDI as acylating reagent to give **1** in 80-85% yield after silica gel column chromatography.

Scheme 1. Synthesis of **1** via the discovery route

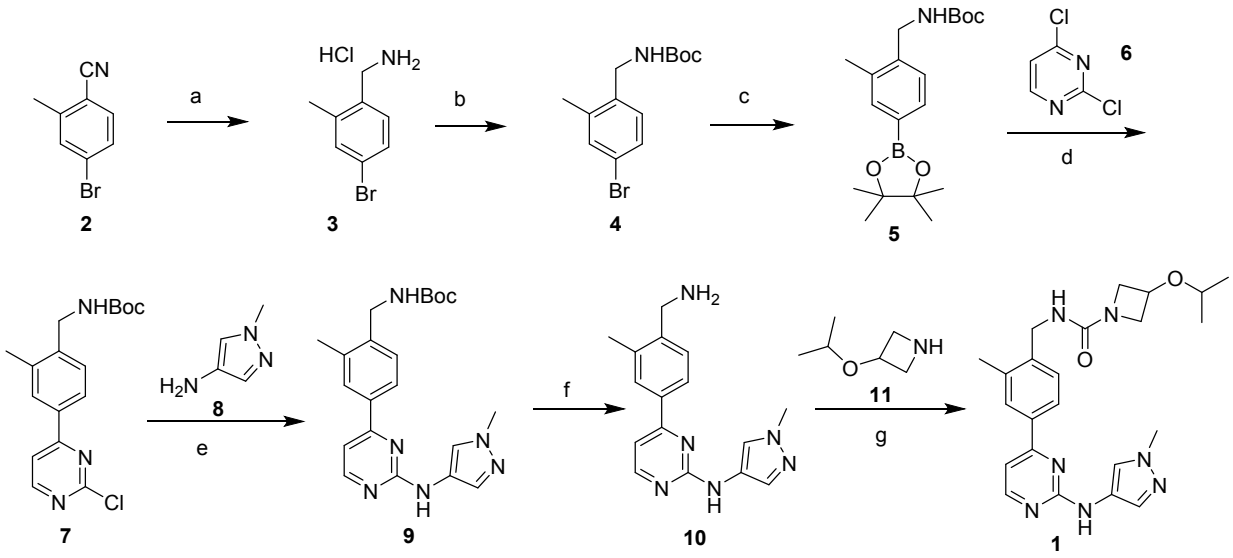

Reagents and conditions: (a) BH_3, THF, 80 °C, 16 h, 90%; (b) Boc_2O, Et_3N, THF, 1 h, 95%; (c) B_2Pin_2, Pd(dppf)Cl_2, KOAc, 1,4-dioxane, 100 °C, 2 h, silica gel column chromatography, 69%; (d) **6**, Pd(dppf)Cl_2, K_2CO_3, 1,4-dioxane:H_2O (4:1), 90 °C, 2 h, silica gel column chromatography, 80%; (e) **8**, $Pd_2(dba)_3$, S-Phos, Cs_2CO_3, 1,4-dioxane, 120 °C, 2 h, silica gel column chromatography, 63%; (f) HCl, MeOH, rt, 6 h, 90%; (g) **11**, CDI, THF, rt, 48 h, silica gel column chromatography, 80-85%. Boc_2O = Di-*tert*-butyl dicarbonate; B_2Pin_2 = Bis(pinacolato)diboron; Pd(dppf)Cl_2 = [1,1′-Bis(diphenylphosphino)ferrocene]dichloropalladium(II); $Pd_2(dba)_3$ = Tris(dibenzylideneacetone)dipalladium(0); S-Phos = 2-Dicyclohexylphosphino-2′,6′-dimethoxybiphenyl; CDI = 1,1′-Carbonyldiimidazole

General Strategy for Process Development to Enable Large-Scale Synthesis. Although the bond disconnection strategy of the medicinal chemistry route to **1** was largely a linear synthesis,[4] it was determined that the discovery synthesis was suitable for the initial kilogram scale preparation of **1** based on the following considerations: (1) timeline constraints to produce drug substance and support toxicology studies, formulation development and Phase I clinical trials; (2) large quantities (> 10 kg) of advanced intermediate **7** had been outsourced and were available for GMP manufacturing; (3) the discovery synthesis was not thoroughly optimized leaving room for process improvement. Therefore, our efforts were focused on the development of final three steps (from **7** to **1**). Our goals were to (1) improve reaction profiles and yields; (2) understand and appropriately control the impurities generated in the process to meet the product quality profile; (3) remove two silica gel column chromatography steps (step **7** to **9** and step **10** to **1**) to enable large-scale production.

Installation of aminopyrazole and *in-situ* Boc deprotection. The first step of the medicinal chemistry route to **1** from intermediate **7** involved a C-N coupling with aminopyrazole **8** using a Pd catalyst. As demonstrated by ample literature precedents, amination of 2-chloropyrimidines can be accomplished under thermal conditions in the presence of either acids[5] or bases,[6] in addition to transition metal catalyzed processes.[7]

1) Reaction optimization: In the event, an initial screening study found that the reaction did not require transition metal[8] (Pd) catalysis or undesirable 1,4-dioxane[9] as solvent (Table 1, entry 1). Although the reaction condition using Cs_2CO_3 without Pd catalyst afforded only 10% desired product **9** (Table 1, entry 2), significant improvement (~ 50%) was realized when K_2CO_3 was

used as base in 1-butanol or NMP (Table 1, entries 4 and 5). When the base was changed to organic bases such as DIEA or Et_3N, the reaction profiles were further improved to ~ 60 % of **9** with ~ 30% of **7** remaining (Table 1, entries 6 and 7).

Advantageously, it was found that under acidic conditions the reaction afforded the desired C-N coupling product and had the added benefit of removing the Boc protecting group in a one-pot process. Initial reaction conditions with 3 equiv of H_3PO_4 in 1-butanol yielded 91% of the de-Boc product **10** (Table 1, entry 8). At this stage of optimization, we examined the HCl salt of **8** as an alternative coupling partner, anticipating the reaction would proceed without additional acid. As expected, the reaction proceeded cleanly giving 92% of **10** (Table 1, entry 10). After optimization of reaction conditions including solvent and temperature, we concluded that heating **8·HCl** salt in 1-butanol at 85 °C was the optimal reaction condition and comparable with reactions at 100 °C (Table 1, entry 11). In this case, the HCl from the **8·HCl** salt and that generated from the displacement reaction was sufficient to promote the Boc deprotection. Formation of of butylated impurity (**14**, Figure 2)[10] under various conditions (Table 1, entries 3 and 4) led us to switch from 1-butanol to 2-butanol. The butylated impurity was not detected when the secondary alcohol was used as reaction solvent, although the reactivity in 2-butanol was found to be lower compared with 1-butanol and 15% of **9** and 9% of **12** remained after 16 h of reaction (Table 1, entry 12). After further optimization, the solvent mixture of 2-butanol/water was found to afford better reactivity than 2-butanol alone (Table 1, entry 13), as the binary solvent enabled a homogenous solution compared with heterogenous reaction mixture when either 1-butanol or 2-butanol was used as single solvent. This homogenous binary solvent system was also ideal for scale-up. The V/V ratio of 2-butanol / water was not critical for the reaction performance and the reaction proceeded well using 2-butanol / water mixture with V/V ratios ranging from 5:2 to 2:3. However, the amount of 2-butanol used had a significant impact on the product loss to the mother liquor. Two volumes of 2-butanol (with respect to the weight of **7)** were used to maximize the isolated yield. An excess of **8·HCl** salt was necessary to drive the reaction to completion. Initially 1.2 equivalents were used, but in an effort to accelerate the reaction the amount of **8·HCl** salt was increased to 1.3 equivalents. Under optimized reaction conditions, different equivalents of **8·HCl** salt were explored (Table 1, entries 13-15) and it was

concluded that 1.3 equivalents of **8·HCl** salt were optimal as more did not give further improvement of reaction profile.

Table 1: Screening results for the C-N coupling of **7** with **8**[a]

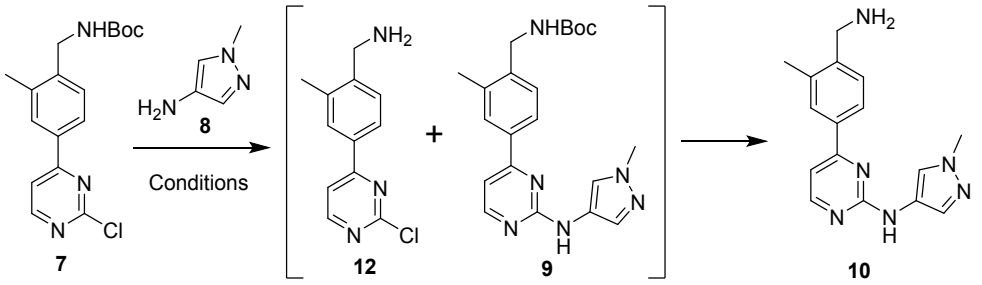

Entry	Reagents	Solvent	Temp	**7** (HPLC A%)	**9** (HPLC A%)	**10** (HPLC A%)
1[b]	$Pd_2(dba)_3$(0.2 equiv), S-Phos(0.1 equiv), Cs_2CO_3 (2 equiv)	1,4-dioxane	100 °C	2	58	0
2	Cs_2CO_3 (2 equiv)	1,4-dioxane	100 °C	67	10	0
3[c]	Cs_2CO_3 (2 equiv)	1-butanol	100 °C	< 1	< 1	< 1
4[d]	K_2CO_3(2 equiv)	1-butanol	100 °C	5	47	< 1
5	K_2CO_3(2 equiv)	NMP	100 °C	25	52	< 1
6	DIEA (2 equiv)	1-butanol	100 °C	31	61	< 1
7	Et_3N (2 equiv)	1-butanol	100 °C	32	60	< 1
8	H_3PO_4 (3 equiv)	1-butanol	100 °C	0	0	91
9	AcOH (3 equiv)	1-butanol	100 °C	0	43	54
10[e]	None	1-butanol	100 °C	0	0	92
11[e]	None	1-butanol	85 °C	0	0	91
12[e,f]	None	2-butanol	85 °C	< 1	15	71

13[e]	None	2-butanol/water (2V/3V)	85 °C	0	0	95
14[e,g]	None	2-butanol/water (2V/3V)	85 °C	0	0	94
15[e,h]	None	2-butanol/water (2V/3V)	85 °C	0	0	93

[a]1.3 equiv of **8** or **8·HCl** salt used for conditions except for entries 14 and 15. All reactions were run for 16 h except for entries 1 and 2 for which the reactions aged for 2 h before analytical samples were taken. [b]Crude reaction contained 15% of **12**. [c]Crude reaction contained 51% of **13** and 28% of **14**. [d] Crude reaction contained 39% of **14**. [e] **8·HCl** salt instead of **8** free base was used for the reactions. [f] Crude reaction mixture contained 9 % of **12**. [g] 1.5 equiv of **8·HCl** salt used. [h] 2.0 equiv of **8·HCl** salt used.

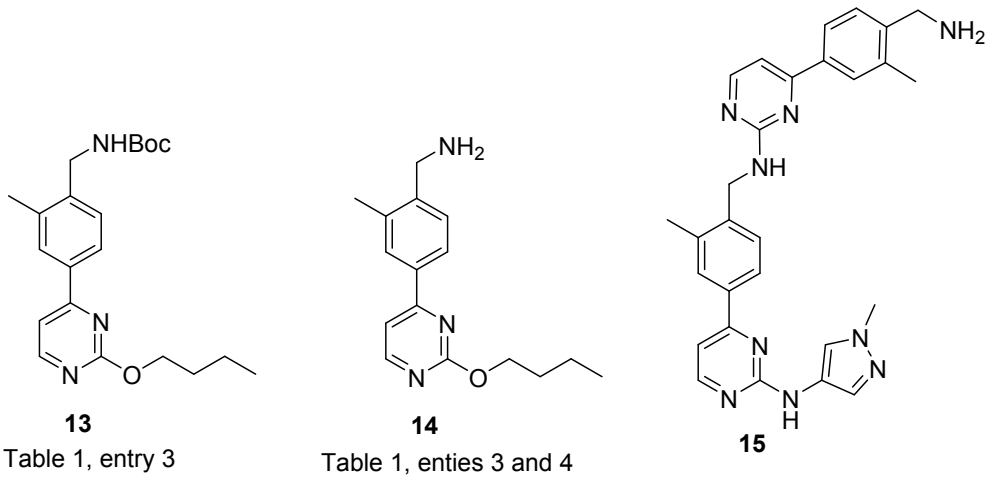

13 Table 1, entry 3 **14** Table 1, enties 3 and 4 **15**

Figure 2. Impurities generated in amination reaction of 2-chloropyrimidine **7** with aminopyrazole **8**

2) Isolation and workup: During process development, it was observed that complete consumption of **12** was necessary before performing the workup. Under basic workup

conditions the chloride on unreacted **12** was displaced by the benzylic amine group of **10** to form a dimer-like side product **15** that did not purge well in the subsequent step. After exploration of various workup conditions, a simple precipitation of **10** free base through the addition of ammonium hydroxide and water was discovered. The workup was originally performed at 20 °C with the addition of ammonium hydroxide followed by dilution with water. This process was complicated with free base **10** precipitating out quickly when the pH of the reaction mixture changed from acidic to basic, resulting in a very thick mixture that was difficult to stir. In order to alleviate this agitation problem, the temperature was increased to 70 °C for the workup, which enabled mixing but resulted in the formation of an unidentified late-eluting impurity. The optimal balance of workability and purity was achieved by decreasing the workup temperature to 35 °C, diluting the reaction mixture with water and the free base was precipitated through addition of ammonium hydroxide. Further optimization resulted in addition of 60% of the total water amount to the reaction followed by addition of a mixture of ammonium hydroxide and the remaining 40% of the water charge, which resulted in isolated **10** in 90 % yield and > 99 % HPLC purity.

Urea formation leading to synthesis of 1. After optimizing the synthesis of benzylamine **10**, we turned our attention to the final chemical bond construction step: the urea formation to generate **1** (Scheme 2).

Scheme 2. Urea synthesis to generate **1**

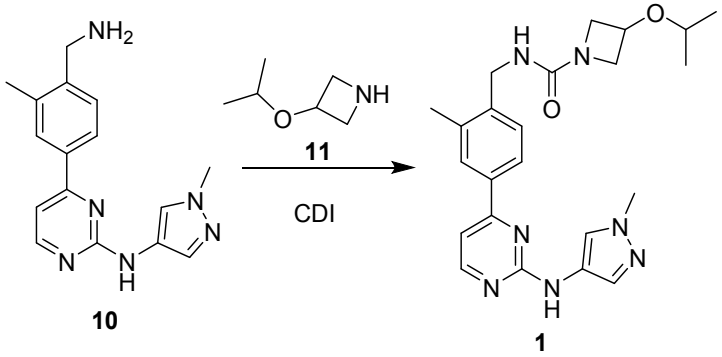

1) **Azetidine:** During development, selection of appropriate form of azetidine starting material was deemed important. 3-Isopropoxyazetidine (**11**) is available as either a solid HCl salt or a

liquid free base. Both forms can be used in the current process; however, the free base provided several advantages over the HCl salt. First, the reaction was noticeably faster with the free base. Second, the HCl salt is extremely hygroscopic and requires special handling. Third, the HCl salt is charged to the reaction as a DMSO solution, while the liquid free base can be conveniently charged into the reaction directly. Finally, a higher level of the chloride ring-opening impurity **16** (Figure 3) was observed when using HCl salt for the reaction suggesting the reaction of **1** with HCl in the matrix. For the current process the use of 3-isopropoxyazetidine (**11**) free base was therefore chosen for development.

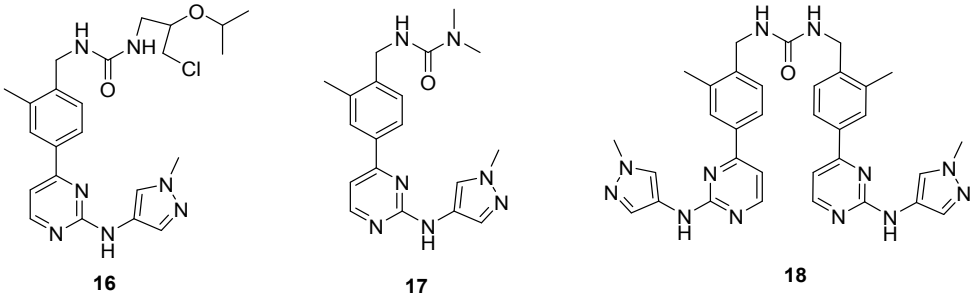

Figure 3: Impurities generated during urea formation step

2) Reaction solvent: The urea formation reaction proceeded in a variety of solvents. Polar aprotic solvents were chosen for scale-up as they fully dissolved all materials and intermediates and eliminated potential stalling observed in some heterogeneous reactions. Although THF was used in the medicinal chemistry route, early toxicology lots were synthesized using two solvents: *N,N*-dimethylformamide (DMF) and dimethylacetamide (DMAc). An impurity associated with DMF (**17**, Figure 3) was tentatively identified by LC-MS; therefore, the solvent was changed to DMAc. However, use of DMAc as the reaction solvent promoted the formation of a bis-addition product **18** (Figure 3). After production of the early toxicology lots, dimethylsulfoxide (DMSO) was determined to be a more suitable solvent providing a cleaner reaction (Table 2, entry 5) with an ICH guideline Class 3 solvent. All **1** prepared for the IND-enabling toxicology studies and clinical studies used DMSO as the solvent for the urea formation step.

3) Bis-addition impurity 18: Unlike impurities **16** and **17**, which can be avoided by using alternative reactants or solvents, a small amount (as low as <1 %) of impurity **18** was observed in all reactions. The impurity level of **18** was linked to 1) the order of addition of **10** and CDI and

2) the CDI equivalents. When a solution of CDI was added to a solution of **10**, impurity **18** was formed in larger amount (Table 2, entries 1-4). The impurity level of **18** was reduced by adding the solution of **10** to the CDI solution over one hour at 30-40°C. Compound **1** made for the IND-enabling toxicology studies and clinical studies used this procedure.

Table 2: Optimization of urea formation step to minimize impurity **17** and **18**[a]

Entry	Solvent	Reaction conditions for mixing 10 with CDI	Product 1[b] (HPLC A%)	Impurity 17 (HPLC A%)	Impurity 18 (HPLC A%)
1	DMF	1.2 equiv of CDI in DMF solution was added to **10** in DMF	92.7	1.8	1.3
2	DMF	**10** in DMF solution was added to 1.2 equiv of CDI in DMF	94.3	1.9	0.7
3	DMAc	0.8 equiv of CDI in DMAc solution was added to **10** in DMAc	73.6	0	21
4	DMAc	**10** in DMAc solution was added to 0.8 equiv of CDI in DMAc	86.5	0	10.2
5	DMSO	**10** in DMSO solution was added to 0.9 equiv of CDI in DMSO	95.8	0	1.4
6	DMSO	**10** in DMSO solution was added to 1 equiv of CDI in DMSO	96.5	0	0.8

7	DMSO	**10** in DMSO solution was added to 1.2 equiv of CDI in DMSO	96.6	0	0.6

a: Reactions were all carried out at 30 °C first by mixing **10** and CDI for < 1 h and then followed by charging **11** and aging for 5 h. b: < 0.5 % HPLC A% of **10** was found in all of the crude reaction mixtures.

Impurity **18** was also formed in much greater quantities when CDI was undercharged. When 0.8 equivalent of CDI was used, the impurity level of **18** reached as high as ~20 % (Table 2, entry 3). Generation of impurity **18** was also observed if CDI decomposed slightly before use. To mitigate this, CDI exposure to air or water was avoided and CDI was stored under refrigeration and an inert atmosphere of nitrogen. On manufacturing scale, the best packaging found to maintain reagent integrity was in unopened, heat sealed, UV protected bags stored under refrigeration. To ensure quality, an extra bag of the reagent having the same lot number was purchased for use in a pre-production use test. The amount of CDI was optimized with DMSO as solvent, it was found that 1.2 equivalent of CDI was sufficient to drive the reaction to completion without significant amount of impurity **18** formation (Table 2, entries 5-7).

Impurity **18** can be removed from **1** by dissolving crude **1** in 10 volumes of ethanol at reflux. The insoluble impurity is removed by hot filtration. This procedure was incorporated in the final co-crystal formation step (see below).

The optimized urea formation procedure was demonstrated at > 100 g scales generating **1** in > 95 % isolated yield and > 99 % HPLC purity.

1 Hemi-Adipate Co-Crystal. As the output of pharmaceutical property assessments with the main goal of improving bioavailability, two salt forms of **1** were identified and characterized as potentially suitable solid forms for further development: the HCl salt and the hemi-adipate co-crystal[11] (**19**). Initial development efforts focused on the HCl salt, however, the chloro-impurity **16** was generated when **1** was treated with HCl. DEREK analysis[12] suggested compound **16** is a potential mutagenic impurity (PMI) and efforts were therefore shifted to the development of the hemi-adipate co-crystal **19**. [13]

Scheme 3: 1 Hemi-Adipate co-crystal formation

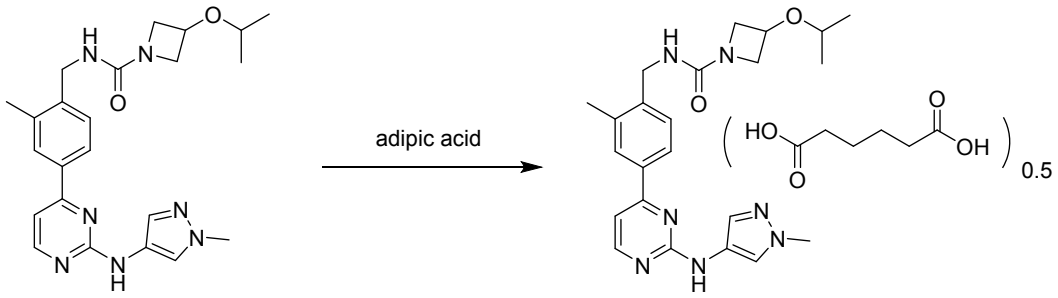

BIIB068 Free Base (**1**) BIIB068 Hemi-Adipate Co-Crystal (**19**)

Both the hemi-adipate co-crystal and mono-adipate co-crystal can be produced. The co-crystals appear loosely bound and both require an excess of adipic acid to crystallize. It was found that isolation of the hemi co-crystal was favored when 0.9-1.1 equiv of adipic acid was used, while the mono-adipate co-crystal was favored with 1.9-2.1 equiv of adipic acid. The hemi-adipate co-crystal was selected for further development.

In the early process evaluation phase, the hemi-adipate co-crystal was readily prepared and precipitated directly via primary nucleation. However, during the development process the purity profile and the composition of the feed stream to the crystallization/co-crystal formation step changed. The new impurity profile inhibited primary nucleation of hemi-adipate, which then could only be produced via seeding and secondary nucleation. To ensure a successful campaign, seeded co-crystal formation was therefore used for production.

The hemi-adipate co-crystal was initially produced in either THF and ethanol. Yield, purity and processing were similar for both solvents. To develop a practical co-crystal formation process, solubility screening was conducted and both **1** and its hemi-adipate (**19**) exhibited high solubility in polar non-protic solvents such as DMSO, DMF and NMP, however, these solvents were found to facilitate disproportionation. Moderate solubility (highly temperature-dependent) was observed in alcohols (methanol, ethanol, 1-propanol, 2-propanol, 1-butanol), 1,4-dioxane, THF, dichloromethane and methyl ethyl ketone. Overall, the solubility screen for **1** and **19** showed alcohol systems (e.g.1-propanol, ethanol, 1-propanol/ethanol mixture) to be most promising for further crystallization development of **1** hemi-adipate. The solubility of both **1** and **19** was acceptable for scale-up, with **19** showing ca. 90-120 mg/mL at 70 °C and less than 10

mg/mL at 5 °C, making a cooling crystallization process feasible. Therefore, ethanol, a Class 3 solvent, was selected for further development.

When ethanol was used as solvent, an ethyl carbamate impurity **20** was generated in the hemi-adipate process. Control experiments found that the unreacted urea intermediate **21** (from urea formation step) in **1** reacts with ethanol in the co-crystal formation step to generate carbamate **20**. To minimize formation of impurity **20** from **21**, the urea formation step was modified to include a residual limit of <0.1% of **21** as well as an increased reaction time or an additional azetidine charge to achieve this limit. Additional lab experiments suggested that **1** also reacted with ethanol to form impurity **20** at a rate of ~ 0.002% per hour at 75 °C. The reaction rate increased significantly with the addition of adipic acid. When adipic acid was present, impurity **21** formed at a faster rate of ~0.01% per hour at 75 °C. To minimize formation of impurity **20** from **1**, the GMP co-crystal formation process was modified so that instead of combining the materials and heating, **1** and the adipic acid were heated separately in ethanol to 75 °C and then combined.

Scheme 4: Formation pathway of ethyl carbamate impurity **20**

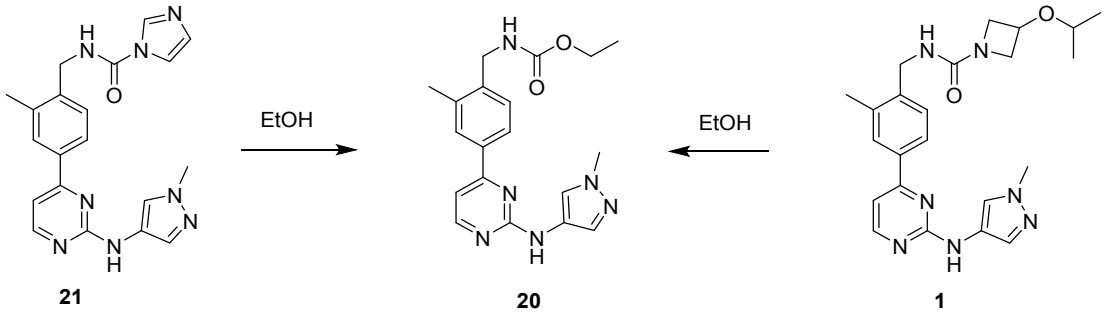

A consistent and reproducible process was thus developed. The reaction was carried out at >70 °C, followed by seeding and crystallization at 60 °C and ramp cooling to 0 °C. The product was isolated by filtration. Slow cooling was found to be essential as rapid cooling causes the mono-adipate co-crystal and/or **1** to precipitate regardless of the use of seeding. The optimized process generated hemi-adipate co-crystal **19** in 90 % yield and > 99 % HPLC purity. The final process is described in the experimental section.

Scale-up Synthesis. The optimized methods described above were used for multi-kilogram synthesis of 1 hemi-adipate co-crystal (**19**). The large-scale manufacturing process effectively reproduced the lab experiments and generated 9.7 kg of **19** with high purity (99.4% by HPLC A%) in excellent overall yield (80 %, table 3). In comparison, the initial medicinal chemistry route generated **1** with 47 % yield from the same starting material **7**. Gratifyingly, two silica gel column chromatography steps in the medicinal chemistry synthesis (**7** to **1**) were successfully removed in the large-scale process.

Table 3: Overview of multi-kilogram synthesis of 1 hemi-adipate co-crystal **19**

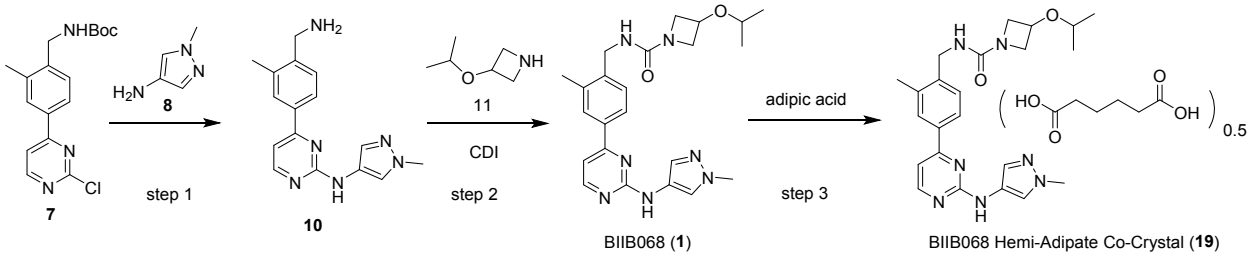

Step	Reaction	Starting weight (kg)	Actual yield (kg)	Yield	Product Purity (HPLC A %)
1	Amination	9.6	7.7	90.0%	99.7%
2	Urea formation	6.6	9.7	99.0%	99.2%
3	Co-crystal formation	9.2	9.7	90.2%	99.4%

Experimental section

Gereral. All reagents and solvents were purchased from commercial suppliers and used without further purification. All reactions were carried out under nitrogen. ^{1}H NMR and ^{13}C NMR spectra were recorded on a Bruker Avance and Varian NMR Spectrometer. Chemical shifts were reported in ppm relative to the residual deuterated DMSO for ^{1}H and ^{13}C, and *J* values were expressed in hertz. The following abbreviations were used to indicate multiplicities: s = singlet; d = doublet; t = triplet; q = quartet; m = multiplet. HPLC analysis was performed on Agilent 1290 instrument. LCMS analysis was performed on Agilent 1290 HPLC+G 6125 MS instrument. XRPD was recorded on DX-2700BH instrument. All yields are uncorrected for purity.

Synthesis of aminopyrazole intermediate 10. To a 22 L RBF (round-bottom flask) 5.0 kg of **8** and 9.2 L (1 vol) of WFI (water for injection) were agitated at 20 °C for 1.5 hours until a homogeneous solution was obtained. To the 200 L GL (glass-lined) reactor 9.6 kg of **7** and 15.6 kg of 2-butanol (2 vol), and 14.6 kg of WFI (2 vol) was charged and warmed at 60 °C for 30 min. The contents of the 22 L RBF were charged over 18 min, rinsing the flask with 5 kg WFI. The reaction mixture was agitated at reflux (83-86 °C) for 19 h, at which point it was complete by HPLC analysis (≤0.05% starting materials/intermediates). The reaction mixture was cooled to 40 °C over 1.75 hours and 46.1 kg WFI (4.8 vol) was charged over 52 min, maintaining 35 ± 5 °C. A mixture of 26.2 kg of 28-30% ammonium hydroxide (7.2 equiv) in 25.7 kg WFI (3.2 vol) was charged over 1 hour 22 min maintaining 35 ± 5 °C, rinsing with 5 kg WFI. The pH of the reaction mixture was measured to be ~11-12 via colorpHast pH paper, cooled to 20.4 °C over 44 min, and held at 15 ± 5 °C for 1 h. The reaction mixture was filtered through a nutsche filter, rinsing the filter cake with 15.4 kg WFI water (1.6 vol). The filter cake (6.9”x17.5”) was loaded onto trays and dried in a vacuum oven at 70 °C. The solids obtained constant weight after 17 hours to afford 7.65 kg **10** in 90 % yield. mp 145.9 °C. ^{1}H NMR (400 MHz, DMSO-d6) δ 9.47 (s, 1H), 8.44 (br d, *J* = 4.8 Hz, 1H), 7. 91 - 7. 94 (m, 3H), 7.53 (br d, *J* = 8.0 Hz, 1H), 7. 22 - 7. 25 (m, 1H), 4.16 (br d, *J* = 6.4 Hz, 1H), 3.82 (s, 3 H), 3.75 (s, 1H), 2.35 (s, 3H). ^{13}C NMR (101 MHz, DMSO-d6) δ163.87, 159.72, 158.81, 144.41, 135.71, 134.73, 129.85, 128.03, 127.35, 124.28, 123.40, 120.31, 106.49, 42.86, 38.68, 18.67. HRMS (ESI) calculated for $C_{16}H_{19}N_6$ $(M + H)^+$ 295.1671, found 295.1653

Synthesis of 1. To a 50 L RBF was charged 22 kg (3 vol) of DMSO and 6.6 kg (22.4 mol) of **10**, warming to 30 ± 5 °C to obtain a homogeneous solution. The % water was measured by KF and the equivalents of CDI was adjusted starting with 1.1 equiv CDI plus water. (This KF suggested 0.14% water which equals 2.2 mol water or 0.096 equiv water). To a 200 L GL reactor was charged 22 kg (3 vol) of DMSO and 4.4 kg (1.198 equiv) of CDI and warm at 30 °C. The solution of **10** in DMSO was charged to the solution of CDI in DMSO slowly over ~1h. The flasks was rinsed with 6.3 kg of DMSO and the reaction mixture was warmed at 30 °C for 30 minutes until the reaction is complete by HPLC (≤1% **10**). 3.4 kg (1.3 equiv) 3-isopropoxyazetidine was charged and the lines were rinsed with 1 kg of DMSO. The reaction mixture was agitated at 30 °C for 4 hours, until completion by HPLC (≤0.10% intermediate). The

reaction mixture was cooled to 20 ± 5 °C and 23.1 kg (3.5 vol) 0 °C water was charged as quickly as possible maintaining ≤ 30 °C. 0.132 kg (2 wt%) **1** freebase seed crystals was immediately charged and the reaction mixture was agitated at a temperature of 20 ± 5 °C to effect crystallization. 23.1 kg (3.5 vol) water was charged slowly over ~1h maintaining ≤ 30 °C and age for 30 minutes at 20 ± 5 °C. Filter the reaction mixture, washing the filter cake 3 x 3 vol water. The solid was dried in a vacuum oven at ≤ 60 °C until ≤ 2% water by KF and ≤ 3% DMSO by GC to afford 9.7kg (99%) **1**. mp 173.7 °C. ^{1}H NMR (400 MHz, DMSO-d6) δ 9.47 (s, 1H), 8.45 (d, *J* = 5.2 Hz, 1H), 7.91 – 7.92 (m, 3H), 7.54 (br s, 1H), 7.35 (br d, *J* = 7.2 Hz, 1H), 7.24 (d, *J* = 5.2 Hz, 1H), 6.85 (t, *J* = 5.8 Hz, 1H), 4.31 - 4.32 (m, 1H) ,4.21 – 4.22 (m, 2H), 4.01 – 4.05 (m, 2H), 3.82 (s, 3H), 3.59 – 3.63 (m, 2H), 3.54 - 3.58 (m, 1H) , 2.36 (s, 3H), 1.07 (d, *J* = 6 Hz, 6H). ^{13}C NMR (101 MHz, DMSO-d6) δ163.81, 159.72, 159.63, 158.90, 141.34, 135.78, 135.17, 129.83, 128.20, 127.45, 124.25, 123.40, 120.31, 106.57, 70.26, 65.11, 57.42, 40.18, 40.80, 40.42, 38.73, 22.31, 18.85. HRMS (ESI) calculated for $C_{23}H_{30}N_7O_2$ $(M + H)^+$ 436.2461, found 436.2427

Preparation of 1 hemi-adipate co-crystal 19. To two 50 L RBFs 36.8 L (4 vol) ethanol and 9.2 kg **1** were charged, while to two 22 L RBFs 27.6L (3 vol) ethanol and 2.8 kg (0.9 equiv) adipic acid were charged. The four flasks were warmed at 70-75 °C and the contents of the 22 L flasks were transferred to the 50L slurries, rinsing with 4.6 L (0.5 vol) ethanol. The flasks were agitated at ~72 °C until a homogenous solution was obtained, then polish filtered into a preheated (70 °C) 200 L GL reactor, rinsing with 4.6 L (0.5 vol) ethanol. Upon reaching an internal temperature of 70 °C, the reaction mixture was agitated 30 min to ensure a homogeneous solution. The reaction mixture was cooled to 62 ± 2 °C and a slurry of 2% seed crystals in saturated **1** ethanol solution was charged, rinsing the lines with 2 L of **1** hemi-adipate saturated EtOH solution. The reaction mixture was gently agitated for 1 h at 60 ± 5 °C to effect crystallization. The reaction mixture was cooled to 5 ± 5 °C over at least 3 h and aged at 5 ± 5 °C for 30 min. The reaction mixture was filtered, washing 3 x 3 vol ethyl acetate, allowing each wash to soak for 15 min. The wet **19** was dried in a vacuum oven until EtOH and EtOAc were both ≤ 5000 ppm by GC to afford 9.67 kg (90.2 %) 1 Hemi-adipate co-crystal **19**. mp 170.7 °C. ^{1}H NMR (400 MHz, DMSO-d6) δ 11.98 (br s, 1H), 9.45 (s, 1H), 8.45 (d, *J* = 4.8 Hz, 1H), 7.91 – 7.92 (m, 3H), 7.55 (br s, 1H), 7.35 (d, *J* = 8.4 Hz, 1H), 7.24 (d, *J* = 5.6 Hz, 1H), 6.83 (t, *J* = 5.6

Hz, 1H) ,4.29 - 4.35 (m, 1H), 4.22 (d, *J* = 5.6 Hz, 2H), 4.02-4.06 (m, 2H), 3.82 (s, 3H), 3.59-3.64 (m, 2H), 3.55 - 3.58 (m, 1H), 2.36 (s, 3H), 2.18 - 2.22(m, 2H), 1.48 - 1.53 (m, 2H) ,1.08 (d, *J* = 6.4 Hz, 6H). ^{13}C NMR (101 MHz, DMSO-d6) δ 174.23, 163.77, 159.70, 159.53, 158.77, 141.22, 135.71, 135.08, 129.84, 128.13, 127.46, 124.15, 123.34, 120.28, 106.50, 70.16, 65.06, 57.34, 40.76, 40.15, 38.63, 33.33, 23.97, 22.22, 18.74. HRMS (ESI) calculated for $C_{23}H_{30}N_7O_2$ $(M + H)^+$ 436.2461, found 436.2427.

AUTHOR INFORMATION

Corresponding Author

Chaomin Li – *Chemical Process Development, Biogen, 225 Binney Street, Cambridge, MA, 02142, United States;* orcid.org/0000-0002-1631-3955;
Email: Chaomin.li@biogen.com

Authors

Lloyd Franklin – *Chemical Process Development, Biogen, 225 Binney Street, Cambridge, MA, 02142, United States*

Robbie Chen – *Chemical Process Development, Biogen, 225 Binney Street, Cambridge, MA, 02142, United States*

Tamera Mack – *Chemical Process Development, Biogen, 225 Binney Street, Cambridge, MA, 02142, United States*

Michael Humora – *Chemical Process Development, Biogen, 225 Binney Street, Cambridge, MA, 02142, United States*

Bin Ma – *Medicinal Chemistry, Biogen, 225 Binney Street, Cambridge, MA, 02142, United States*

Brian T. Hopkins – *Medicinal Chemistry, Biogen, 225 Binney Street, Cambridge, MA, 02142, United States*

John Guzowski – *Chemical Process Development, Biogen, 225 Binney Street, Cambridge, MA, 02142, United States*

Fengmei Zheng – *Pharmaceutical Sciences, Biogen, 225 Binney Street, Cambridge, MA, 02142, United States*

Michael MacPhee – *Pharmaceutical Sciences, Biogen, 225 Binney Street, Cambridge, MA, 02142, United States*

Yiqing Lin – *Pharmaceutical Sciences, Biogen, 225 Binney Street, Cambridge, MA, 02142, United States*

Steven Ferguson – *Chemical Process Development, Biogen, 225 Binney Street, Cambridge, MA, 02142, United States*

Daniel Patience – *Chemical Process Development, Biogen, 225 Binney Street, Cambridge, MA, 02142, United States*

George A. Moniz – *CMC Management, Biogen, 225 Binney Street, Cambridge, MA, 02142, United States*
William F. Kiesman – *Chemical Process Development, Biogen, 225 Binney Street, Cambridge, MA, 02142, United States*
Erin M. O'Brien – *Chemical Process Development, Biogen, 225 Binney Street, Cambridge, MA, 02142, United States*

Complete contact information is available at:

Notes

The authors declare no competing financial interest.

ACKNOWLEDGEMENTS

We thank Cuicui Yuan, Deju Shang, Dong Wang, Ruiling Wang and Yinli Wu (WuXi Chemical Service Unit) for experimental assistance, Yiqiong Guo and Miaomiao Xie (WuXi Core Analytical Service) for analytical support.

SUPPORTING INFORMATION

The supporting information is available free of charge on the ACS publication website at DOI:

Content of supplementary material: 1) General Information; 2) Analytical Spectra of **10**, **1** and **19**; 3) Analytical Spectra of Impurities; 4) Analytical Spectra of Reaction Optimization (**7** to **10**, table 1); 5) Single Crystal Structure of **19.**

REFERENCES

[1] (a) Kim, H. Development of BTK inhibitors for the treatment of B-cell malignancies. *Arch. Pharmacal Res.* **2019**, *42* (2), 171-181. (b) Xia, B.; Qu, F.; Yuan, T.; Zhang, Y., Targeting Bruton's tyrosine kinase signaling as an emerging therapeutic agent of B-cell malignancies. *Oncol. Lett.* **2015**, *10* (6), 3339-3344.
[2] (a) Lv, J.; Wu, J.; He, F.; Qu, Y.; Zhang, Q.; Yu, C. Development of Bruton's Tyrosine Kinase Inhibitors for Rheumatoid Arthritis. *Curr. Med. Chem.* **2018**, *25* (42), 5847-5859. (b) Liang, C.; Tian, D.; Ren, X.; Ding, S.; Jia, M.; Xin, M.; Thareja, S. The development of Bruton's tyrosine kinase (BTK) inhibitors from 2012 to 2017: A mini-review. *Eur. J. Med. Chem.* **2018**, *151*, 315-326.
[3] A separate manuscript discussing medicinal chemistry research is in preparation.

[4] Dach, R.; Song, J.; Roschangar, F.; Samstag, W.; Senanayake. C. The Eight Criteria Defining a Good Chemical Manufacturing Process. *Org. Process Res. Dev.* **2012**, *16*, 1697−1706.

[5] Selected examples of acid promoted amination of 2-chloropyrimidines: (a) Mishra, N. K.; Choi, M.; Jo, H.; Oh, Y.; Sharma, S.; Han, S. H.; Jeong, T.; Han, S.; Lee, S-Y; Kim, I. S. Direct C–H alkylation and indole formation of anilines with diazo compounds under rhodium catalysis. *Chemical Communications* (Cambridge, United Kingdom), **2015**, *51* (97), 17229-17232 (b) Maddess, M.; Carter, R. SNAr reactions of 2-methylthio-4-pyrimidinones in pivalic acid: access to functionalized pyrimidinones and pyrimidines. *Synthesis*, **2012**, *44* (7), 1109-1118.

[6] Selected examples of base promoted amination of 2-chloropyrimidines: (a) Gill, D.; Iveson, M.; Collins, I.; Jones, A. A Mitsunobu reaction to functionalized cyclic and bicyclic N-arylamines. *Tetrahedron Letters*, **2018**, *59* (3), 238-242 (b) Ho, L.; Raston, C.; Stubbs, K. Transition-Metal-Free Cross-Coupling Reactions in Dynamic Thin Films To Access Pyrimidine and Quinoxaline Analogues. *European Journal of Organic Chemistry*, **2016**, *36*, 5957-5963.

[7] (a) Zhang, G.; Wang, X.; Li, C.; Yin, D. Palladium-Catalyzed Cross-Coupling of Electron-Deficient Heteroaromatic Amines with Heteroaryl Halides. *Synthetic Communications*, **2013**, *43* (3), 456-463 (b) Shaw, J.; Grayson, D.; Rozas, I. Synthesis of cyclic guanidines: 2-arylamino-1,4,5,6-tetrahydropyrimidines. *ARKIVOC* (Gainesville, FL, United States), **2014**, (2), 161-174 (c) Zhang, H.; Xia, Z.; Vasudevan, A.; Djuric, S. Efficient Pd-catalyzed synthesis of 2-arylaminopyrimidines via microwave irradiation. *Tetrahedron Lett.* **2006**, *47* (28), 4881-4884.

[8] Bryan, M.; Dunn, P.; Entwistle, D.; Gallou, F.; Koenig, S.; Hayler, J.; Hickey, M.; Hughes, S.; Kopach, M.; Moine, G.; Richardson, P.; Roschangar, F.; Steven, A.; Weiberth. F. Key Green Chemistry research areas from a pharmaceutical manufacturers' perspective revisited. *Green Chem.*, **2018**, *20*, 5082.

[9] 1,4-Dioxane is class 2 solvent (solvents to be limited) based on ICH Q3C with permitted daily exposure of 3.8 mg/day.

[10] ~ 0.4 % of **14** was observed for entry 11 reaction.

[11] Initially the hemi-adipate form was named hemi-adipate salt, however, based on the calculated pKa of 2.75 it is very likely that the adipate is a co-crystal. Single crystal structure of hemi-adipate was later obtained and co-crystal form was therefore confirmed. see MacPhee, M.; Chen, R.; Ferguson, S.; Franklin, L.; Mack, T. Preparation of adipate forms and compositions of biaryl inhibitors of Bruton's tyrosine kinase. *PCT Int. Appl.* **2016**, WO 2016201271 A1, December 15, 2016.

[12] DEREK (Deductive Estimation of Risk from Existing Knowledge) is an expert rule-based computer modelling program developed by Lhasa (Oxford, UK) designed for computational toxicological assessments. Also see (a) Greene, N.;Judson, P.; Langowski. J.; Marchant, C. Knowledge-based expert systems for toxicity and metabolism prediction: DEREK, StAR and METEOR. *SAR QSAR. Environ. Res.***1999**, *10*, 299–314. (b) Dobo, K.; Greene, N.; Fred, C.; Glowienke, S.; Harvey, J.; Hasselgren, K.; Jolly, R.; Kenyon, M.; Munzner, J.; Muster, W.; Neft, R.; Reddy, V.; White, A.; Weiner, A. In silico methods combined with expert knowledge rule out mutagenic potential of pharmaceutical impurities: An industry survey. *Regul. Toxicol. Pharmacol.* **2012**, *62*, 449–455. (c) Galloway, S.; Reddy, V.; McGettigan, K.; Gealy, R.; Bercu, J. Potentially mutagenic impurities: Analysis of structural classes and carcinogenic potencies of chemical intermediates in pharmaceutical syntheses supports alternative methods to the default TTC for calculating safe levels of impurities. *Regul. Toxicol. Pharmacol.* **2013**, *66*, 326–335.

[13] MacPhee, M.; Humora, M. Preparation of forms and compositions of biaryl inhibitors of Bruton's tyrosine kinase. *PCT Int. Appl.* **2016**, WO 2016201280 A1, December 15, 2016.